Electronic Supplementary Material (ESI) for Nanoscale.

The effect of pressure on the post-synthetic modification of a nanoporous metal-organic framework

Scott C. McKellar[a], Alexander J. Graham[a], David R. Allan[b], M. Infas H. Mohideen[c], Russell E. Morris[c] and Stephen A. Moggach*[a]

[a]EaStCHEM School of Chemistry and the Centre for Science at Extreme Conditions, University of Edinburgh, Kings Buildings, West Mains Road, Edinburgh, EH9 3JJ, UK.
[b]Diamond Light Source Ltd, Diamond House, Harwell Science and Innovation Campus, Oxfordshire, OX11 0DE, UK.
[c]EaStCHEM School of Chemistry, University of St Andrews, Purdie Building, St Andrews, KY16 9ST, UK.

Supplementary Information

All raw materials were purchased from Sigma-Aldrich (UK) in high purity and used as received.

Synthesis of STAM-1 ($Cu(C_{10}H_6O_6)(H_2O).1.66H_2O$)[1]

$Cu(NO_3)_{2\cdot3}(H_2O)$ and 1,3,5-benzenetricarboxylic acid (H_3BTC) were mixed with $MeOH/H_2O$ (50:50) in a Teflon-lined steel autoclave. The mixture was then heated at 383 K for 7 days. The autoclave was cooled to room temperature, and large blue crystals were isolated by Buchner filtration and dried in air.

Synthesis of HKUST-1 ($Cu_3(BTC)_2(H_2O)_3$)

HKUST-1 was synthesised as per a previously described method.[2]

High-pressure single-crystal X-ray diffraction experiments

General procedures

High-pressure experiments were carried out using a modified Merrill-Bassett diamond anvil cell (DAC) equipped with 600 μm culet diamonds and a tungsten gasket.[3] The sample and a chip of ruby (as a pressure calibrant) were loaded into the DAC using one of six hydrostatic media; methanol (MeOH), ethanol (EtOH), isopropyl alcohol (IPA), acetonitrile (MeCN), acetaldehyde (ethanal; MeCHO) and water. The ruby fluorescence method was used to measure the pressure.[4]

Data collection, reduction and refinement

Before each pressure study (and after if crystal recovery was possible) an ambient pressure and temperature single-crystal X-ray diffraction data set was collected on a Bruker APEXII diffractometer (Bruker, 2002) with graphite-monochromated Mo *K*α radiation (λ = 0.71073 Å). These data were integrated using the programme SAINT[5], while the absorption corrections were carried out with the program SADABS[6]. Refinements were carried out against $|F|^2$ using all data in CRYSTALS[7]. Pore volume and water content were calculated using the SQUEEZE algorithm within PLATON[8]. Refinement was carried out against $|F|^2$ using all data[9] starting from the ambient temperature coordinates of Mohideen *et al*.[1]

High-pressure single-crystal X-ray diffraction data of STAM-1_{MeOH} and STAM-1 in IPA were collected on beamline I19 at the DIAMOND Light Source (λ = 0.4859 Å). Data were

collected in ω-scans in eight settings of 2θ and ϕ with a frame time and step size of one second and 0.5° respectively. This data collection strategy was based on that described by Dawson *et al*.[10] Diffraction data of STAM-1_{MeCN}, STAM-1 in MeCHO and H_2O and HKUST-1 in H_2O were collected on the Bruker APEXII lab source described above with a frame time of 30-60 seconds, depending on the sample. The data were integrated using the program SAINT using 'dynamic masks' to avoid integration of regions of the detector shaded by the body of the pressure cell.[10] Absorption corrections for the DAC and sample were carried out with the programs SHADE[11] and SADABS respectively.

Compression study using isopropyl alcohol (IPA)

A crystal of STAM-1 was loaded in a DAC with IPA at 0.5 GPa. Data were collected in approximately 0.5 GPa steps up to 2.4 GPa. On increasing pressure from 0.9 to 1.5 GPa, the crystal started to break up, and the resolution deteriorated rapidly. As a result, unit cell dimensions could only be reported above 0.9 GPa. Above 2.40 GPa, the sample became polycrystalline and no further information could be extracted. Refinements of STAM-1 were carried out against $|F|^2$ using all data.[9] Because of the low completeness of the data-sets, all 1,2 and 1,3 distances on the monomethyl benzene-1,3,5-tricarboxylic acid linker were restrained to the values observed from our ambient temperature and pressure structure. All metal-ligand distances and angles, and all torsion angles were refined freely. Thermal and vibrational similarity restraints were applied to the organic linker. H-atoms attached to carbon were placed geometrically and not refined. The water H-atoms were initially found in a difference map and refined with a bond length restraint to regularise its geometry (rO-H = 0.82(1) Å) with U[iso] set to 1.2 times U[eq] of the parent atom. On converging, all H-atoms were refined with riding constraints.

Compression study using methanol (MeOH)

Upon loading STAM-1 in a DAC with MeOH to 0.2 GPa, a ligand exchange reaction was observed. This new form of STAM-1 is hereafter referred to as STAM-1_{MeOH}. The reaction involved exchange of methanol for water at the axial coordination site of the Cu^{II} dimer. The structure of STAM-1_{MeOH} was determined by starting from the ambient pressure coordinates of STAM-1 by Mohideen *et al*. The methyl group position was determined by a difference Fourier map. In order to ascertain whether STAM-1_{MeOH} was stable at room temperature, the

same crystal was recovered to ambient pressure and temperature, and a single-crystal X-ray diffraction data set was then collected.

In a separate high-pressure study, another crystal of STAM-1 was loaded into a DAC with methanol to 0.5 GPa and high-pressure data were collected in approximately 0.9 GPa steps up to 5.7 GPa. Refinements of STAM-1_{MeOH} were carried out against $|F|^2$ using all data.[9] Because of the low completeness of the data-sets, all 1,2 and 1,3 distances on the monomethyl benzene-1,3,5-tricarboxylic acid linker and MeOH ligand were restrained to the values observed from our ambient temperature and pressure structure. All metal-ligand distances and angles, and all torsion angles were refined freely. Thermal and vibrational similarity restraints were applied to both the organic linker and MeOH ligand. H-atoms attached to carbon were placed geometrically and not refined. The H-atom attached to the oxygen atom were initially found in a difference map and refined with restraints on the bond length to regularise its geometry (O-H = 0.82 Å) with U[iso] set to 1.2 times U[eq] of the parent atom. On converging, all H-atoms were refined with riding constraints. Above 5.73 GPa, the crystal broke apart, becoming polycrystalline.

Compression study using acetonitrile (MeCN)

Upon loading STAM-1 in a DAC with MeCN to 0.3 GPa, a ligand exchange reaction was observed. This new form of STAM-1 is hereafter referred to as STAM-1_{MeCN}. The reaction involved exchange of MeCN for water at the axial coordination site of the Cu^{II} dimer. The structure of STAM-1_{MeCN} was determined by starting from the ambient pressure coordinates of STAM-1 by Mohideen *et al*. The MeCN position was determined by a difference Fourier map. The occupancy of the MeCN ligand was one third, while water in the same position had an occupancy of two thirds. In order to ascertain whether STAM-1_{MeCN} was stable at room temperature, the same crystal was recovered to ambient pressure at 150 K, and a single-crystal X-ray diffraction data set was then collected. The temperature was then increased to room temperature and a further data set was collected. In a separate high-pressure study, another crystal of STAM-1 was loaded into a DAC with MeCN to 0.5 GPa, but the hydrostatic medium froze at this pressure so no further data could be collected.

Refinements of STAM-1_{MeCN} were carried out against $|F|^2$ using all data for ambient-pressure structures and $|F|$ with an $I>2\sigma$ cut off for high-pressure structures.[9] Because of the low completeness and lack of high-angle data in the data-sets, and part-occupancy of the ligand,

all distances and angles on the MeCN ligand, including the metal-ligand distance, were restrained. Thermal and vibrational similarity restraints were applied to both the organic linker and MeCN ligand. H-atoms attached to carbon were placed geometrically and not refined. The water H-atoms were initially found in a difference map and refined with a bond length restraint to regularise its geometry (rO-H = 0.82(1) Å) with U[iso] set to 1.2 times U[eq] of the parent atom. On converging, all H-atoms were refined with riding constraints.

Compression study using acetaldehyde (MeCHO)

A crystal of STAM-1 was loaded in a DAC with MeCHO at 0.6 GPa. Due to the low boiling point of MeCHO (20.2°C), the solvent was kept below room temperature and loaded while the DAC was kept on an electronic ice cube. However, due to the volatility of the solvent, the gasket hole was not filled completely, and thus the gasket hole shrank when pressure was applied. This resulted in problems with gasket shading during collection of diffraction data, namely a reduction in the number of unique reflections. This severely impacted on the quality of the crystal structure. To maximise the data:parameter ratio, the STAM-1 structures in MeCHO were only refined isotropically. The reduction in gasket hole size also accounts for the large jumps in pressure over the course of the pressure series (see Table S4), since even tiny turns of the DAC screws yielded a disproportionately large pressure increase. The structure of STAM-1 was determined by starting from the ambient pressure coordinates of STAM-1 previously obtained. Data were collected in approximately 1 GPa steps up to 5.4 GPa. On increasing pressure above 3 GPa, the data resolution deteriorated significantly and as a result, only unit cell dimensions could be reported. Above 5.4 GPa, the sample became amorphous and no further information could be extracted. Refinements of STAM-1 were carried out against $|F|$ using data with $I>2\sigma$.[9] Because of the low completeness of the data-sets, all 1,2 and 1,3 distances on the monomethyl benzene-1,3,5-tricarboxylic acid linker were restrained to the values observed from our ambient temperature and pressure structure. All metal-ligand distances and angles, and all torsion angles were refined freely. Thermal and vibrational similarity restraints were applied to the organic linker. H-atoms attached to carbon were placed geometrically and not refined. The water H-atoms were not modelled. On converging, all H-atoms were refined with riding constraints.

Due to the low data:parameter ratio, the accuracy of the pore volume and content calculated for STAM-1 in MeCHO is diminished. Quoted values in Table S4 are thus more subject to error. The resolution of each data set is 0.9 Å at 0.7 GPa, 1 Å at 2.0 GPa and 1.05 Å at 3.0

GPa. We have also artificially reduced the resolution of each data set and performed PLATON *SQUEEZE* analysis, which shows little change in the calculated values (Table S4). Therefore, though the values may have a higher inherent error, we believe the trend is correct, and that there is a gating pressure of STAM-1 in MeCHO around 2 GPa which results in the pore-emptying phenomenon discussed.

Compression study using water

A crystal of STAM-1 was loaded in a DAC with water at 0.1 GPa and X-ray diffraction data were collected. The structure was determined by starting from the ambient pressure coordinates of STAM-1 previously determined. On increasing pressure further, the crystal decomposed and needle-like crystals were observed growing from the edge of the crystal. No further information could be extracted. Refinements of STAM-1 were carried out against $|F|$ using data with $I>2\sigma$.[9] Because of the low completeness of the data-sets, thermal and vibrational similarity restraints were applied to the organic linker. H-atoms attached to carbon were placed geometrically and not refined. On converging, all H-atoms were refined with riding constraints. Disordered water in the cavity was modelled isotropically with part-occupancies as calculated in CRYSTALS. The water H-atoms were not modelled.

Compression study of HKUST-1 using water

A crystal of HKUST-1 as loaded in a DAC with water at 0.2 GPa and X-ray diffraction data were collected. The structure of STAM-1_{MeCN} was determined by starting from the ambient pressure coordinates of HKUST-1 by Graham *et al*.[12] On increasing pressure further, the crystal started to break up, and the resolution deteriorated rapidly. As a result, only unit cell dimensions could be reported above 0.2 GPa. Above 0.4 GPa, the sample became polycrystalline and no further information could be extracted. Refinements of HKUST-1 at 0.2 GPa were carried out against $|F|$ using data with $I>2\sigma$.[9] H-atoms attached to carbon were placed geometrically and not refined. On converging, all H-atoms were refined with riding constraints. The water H-atoms were not modelled.

Ambient-pressure single-crystal X-ray diffraction experiments

Diffraction in a capillary with liquid

A crystal of STAM-1 was stuck to the tip of a MiTeGen 100 μm Microloop™ using a small amount of Araldite™ epoxy resin. The loop was mounted on a goniometer head, and covered with a MicroRT™ polyester capillary. The capillary was stuck to the goniometer head and sealed around the base using Araldite™. When the epoxy resin was dry, the capillary was filled with MeOH by injecting the solvent through the top of the capillary using a 0.6 mm needle. The resultant hole was sealed by melting a small amount of beeswax over the hole. Diffraction data were then collected and processed as previously described. Despite a high background due to absorption by the liquid, the crystal structure was able to be solved using the SUPERFLIP charge flipping algorithm[13], which confirmed the sample to be STAM-1_{MeOH}.

The above was repeated using EtOH and MeCN. With EtOH, the crystal broke apart on the mount, preventing data collection. The crystal structure solved in MeCN confirmed that the ligand exchange reaction had not occurred.

Reaction of STAM-1 with amines

A small spatula tip of STAM-1 crystals was added to a 3 mL glass vial. 2 mL of 2.0 M solution of methylamine ($MeNH_2$) in THF was added to the vial and left uncovered. As the oil-like sample dried, a small crystal was able to be extracted from the vial and X-ray diffraction data were collected at 150 K, and then again at room temperature. Data was collected, processed and refined as described previously for ambient-pressure experiments. This process was repeated using ethylamine ($EtNH_2$) and *n*-propylamine ($PrNH_2$) as solvents.

A ligand exchange reaction analogous to STAM-1_{MeCN} was observed for both $MeNH_2$ and $EtNH_{2\ in}$ the crystal structures at 150 K. These new forms of STAM-1 are hereafter referred to as STAM-1_{MeNH2} and STAM-1_{EtNH2}. The reaction involved exchange of the amines for water at the axial coordination site of the Cu^{II} dimer. The structures of STAM-1_{MeNH2} and STAM-1_{EtNH2} were solved using SUPERFLIP. The amine ligand positions were determined by a difference Fourier map. The occupancy of each ligand was one third, while water in the same position had an occupancy of two thirds. No exchange was detected for STAM-1 in $PrNH_2$.

Refinements of STAM-1_{MeNH2} and STAM-1_{EtNH2} were carried out against $|F|^2$ using all data.[9] Because of the lack of high-angle data and part-occupancy of the ligand, distances and angles on the amine ligands were restrained where necessary. Thermal and vibrational similarity restraints were applied to both the organic linker and amine ligands. H-atoms attached to carbon were placed geometrically and not refined. The water H-atoms and amine H-atoms were assumed to occupy the same position, and were initially found in a difference map and refined with a bond length restraint to regularise its geometry (rO-H = 0.82(1) Å) with U[iso] set to 1.2 times U[eq] of the parent atom. On converging, all H-atoms were refined with riding constraints.

Software for structure analysis

Crystal structures were visualized using the programs DIAMOND[14] and MERCURY.[15] Void analyses carried out in MERCURY used the contact surface with a probe radius of 1.2 Å and an approximate grid spacing of 0.7 Å unless otherwise specified.

Structure of STAM-1

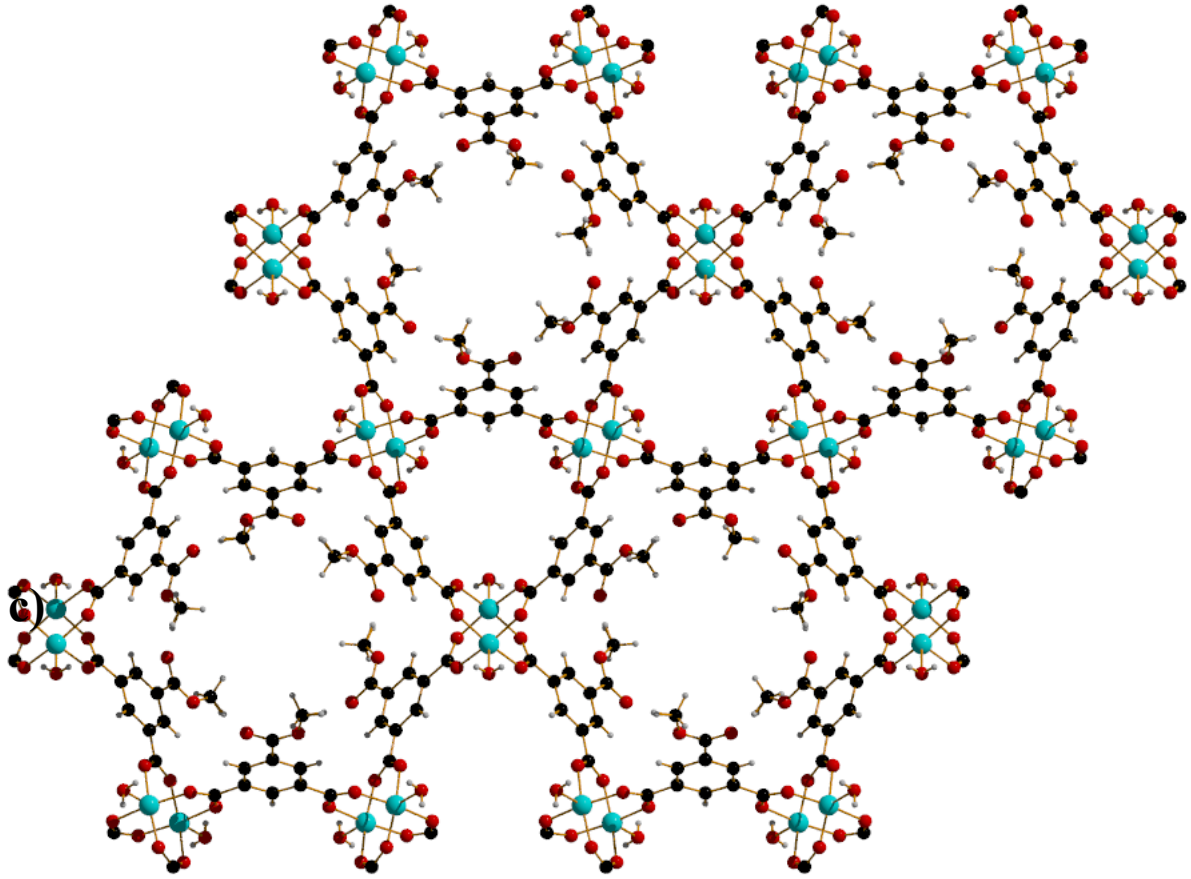

Figure S1 Overall structure of STAM-1 viewed parallel to the crystallographic *c*-axis, showing hydrophobic channels lined by ester groups and the hydrophilic channel lined by coordinated water molecules. Key: Cu, turquoise; O, red; C, black; H, white.

Table S1. Abridged crystallographic data and structure refinement parameters for native STAM-1

	STAM-1
empirical formula	$C_{30}H_{34}Cu_3O_{26}$
temperature (K)	300
wavelength (Å)	0.71073
crystal system	trigonal
space group	$P\bar{3}m1$
a (Å)	18.6500(17)
b (Å)	18.6500(17)
c (Å)	6.8329(9)
α (°)	90
β (°)	90
γ (°)	120
volume (Å^3)	2058.2(4)
Z	2
density (g cm^{-3})	1.557
absorption coefficient (mm^{-1})	1.611
F(000)	918.0
θ range (°)	1.3 – 28.4
index ranges	$-21 \leq h \leq 0$
	$0 \leq k \leq 24$
	$0 \leq l \leq 9$
reflections collected	22534
independent reflections	1832
	[R(int) = 0.042]
data / restraints / parameters	1832 / 4 / 96
goodness-of-fit on F^2	0.9395
Final R indices [$I > 2\sigma(I)$]	$R_1 = 0.032$
	$wR_2 = 0.081$
R indices (all data)	$R_1 = 0.045$
	$wR_2 = 0.085$
largest difference peak (eÅ^{-3})	0.54
deepest hole (eÅ^{-3})	-0.61

Structure of STAM-1$_{MeOH}$

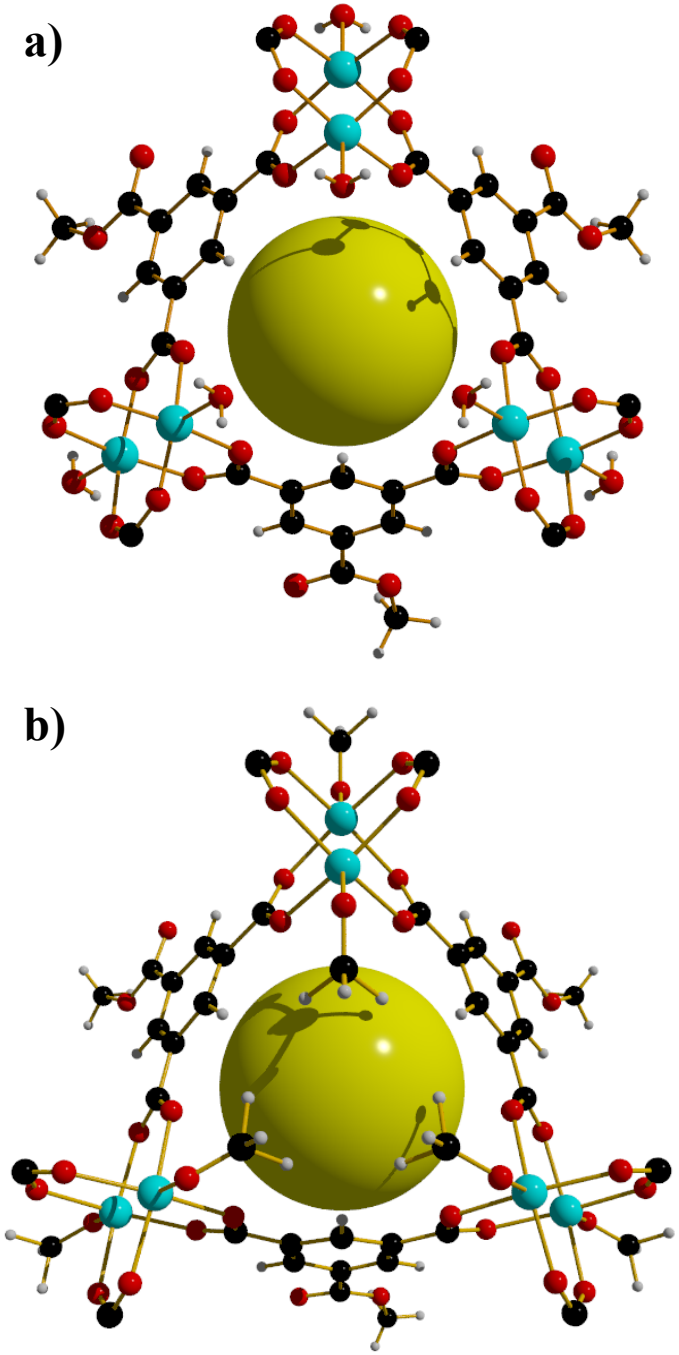

Figure S2. a) One of the cup-like structural units found in STAM-1 viewed along the *c*-axis, showing the hydrophilic nature of the pore. The yellow sphere is illustrative only and set to a diameter of 2.75 Å. **b)** The equivalent cup-like structure found in STAM-1$_{MeOH}$ viewed along the *c*-axis. The chemical nature of the pore has been altered by the introduction of the coordinated methanol. The methyl groups also hinder the movement of guest through the 1D channel.

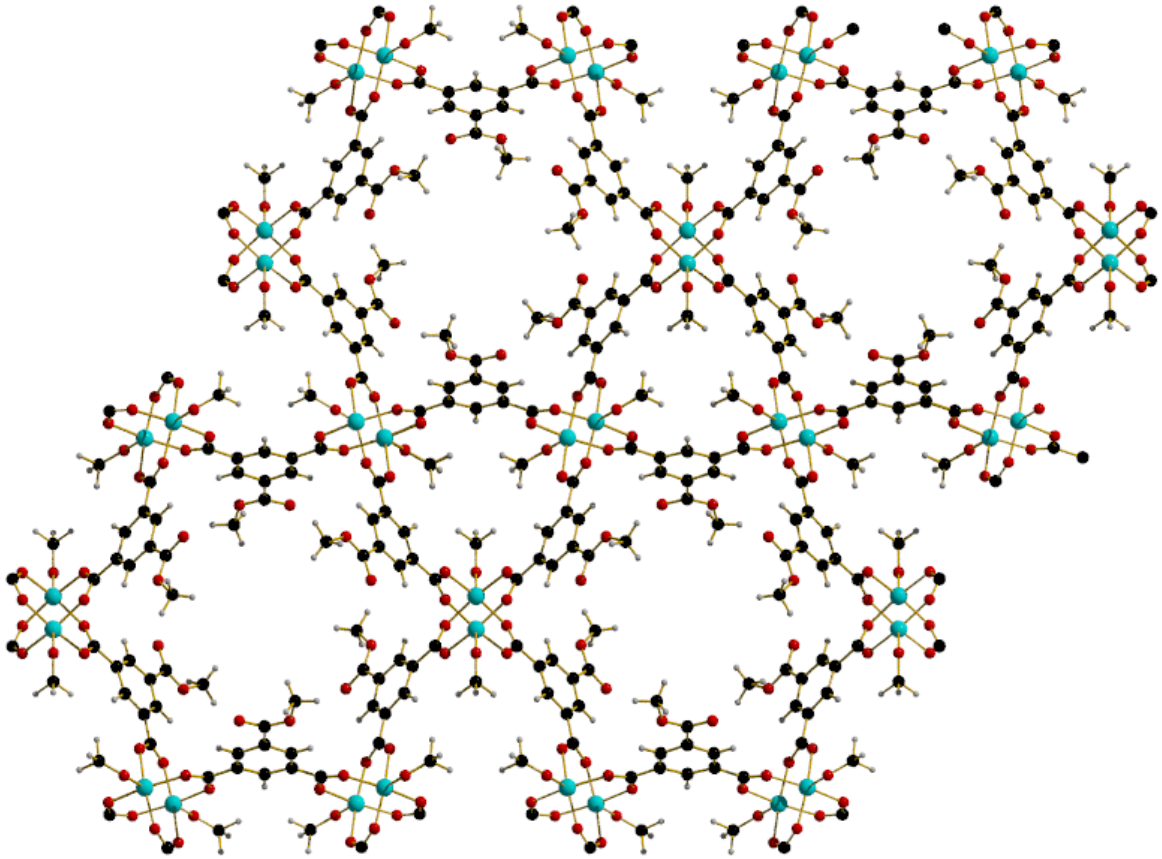

Figure S3. Overall structure of STAM-1_{MeOH} viewed parallel to the crystallographic *c*-axis, showing the original hydrophobic channels lined by ester groups. The previously hydrophilic channels are now lined by exchanged methanol moieties that change the chemical and steric nature of the channel.

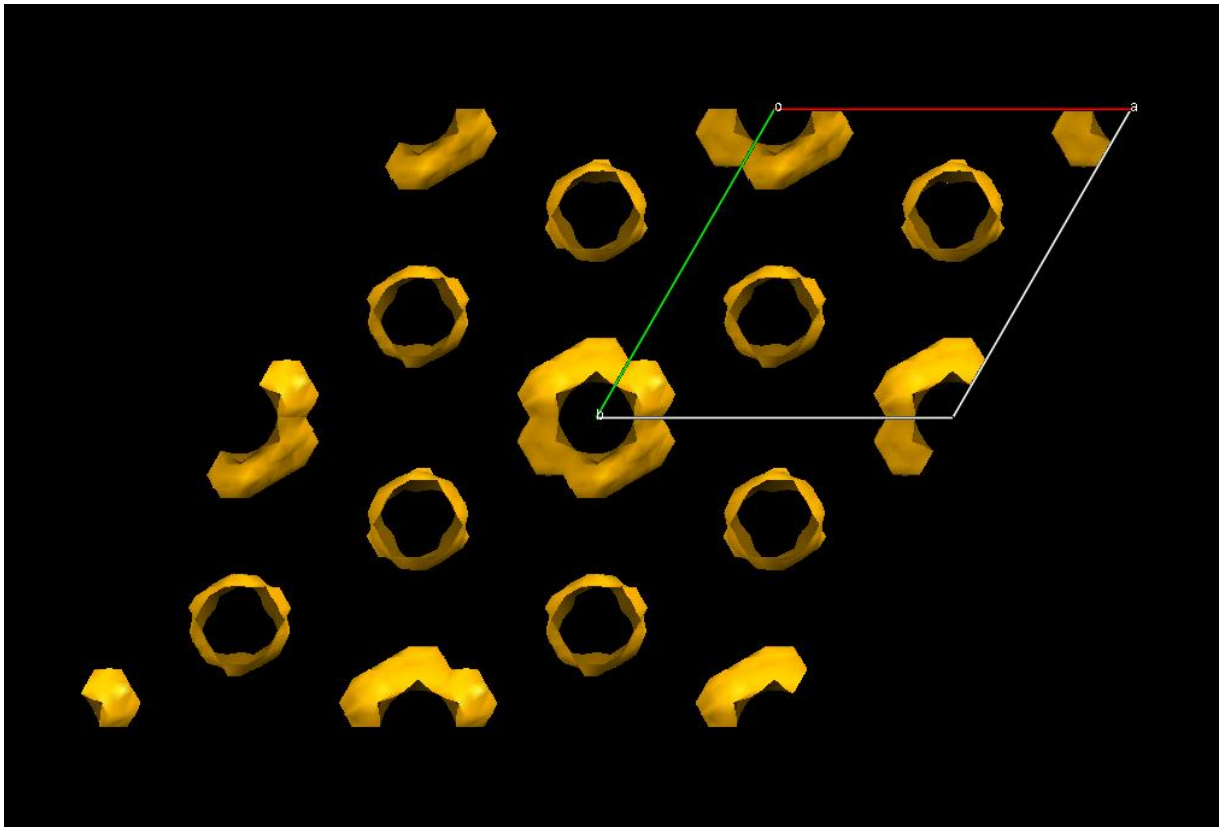

Figure S4. Void spaces of STAM-1 at ambient pressure and temperature. Six smaller hydrophilic channels surround every larger hydrophobic pore.

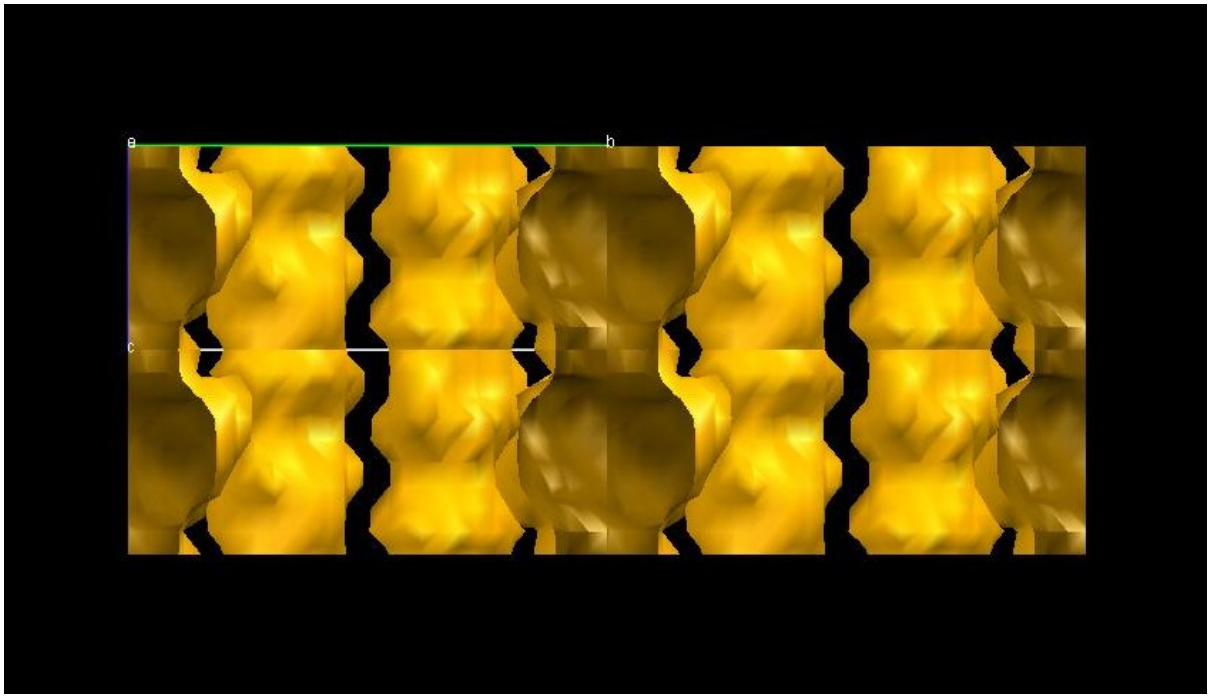

Figure S5. STAM-1 contact surface as calculated in MERCURY, viewed along the crystallographic *a*-axis. The hydrophobic pores are located in the centre and on the extreme left and right of the figure. The hydrophilic channels are located between the hydrophobic pores.

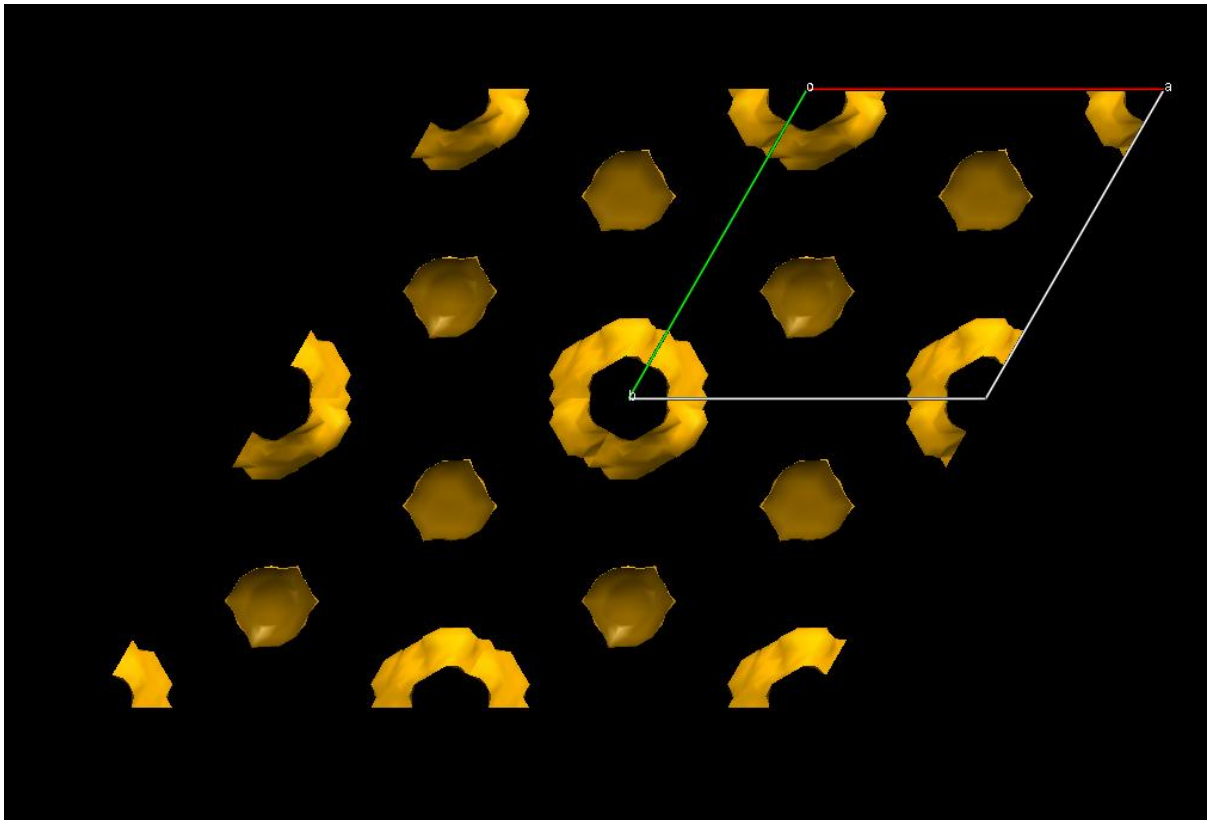

Figure S6. STAM-1_{MeOH} contact surface as calculated in MERCURY. The previously hydrophobic pores are now effectively closed.

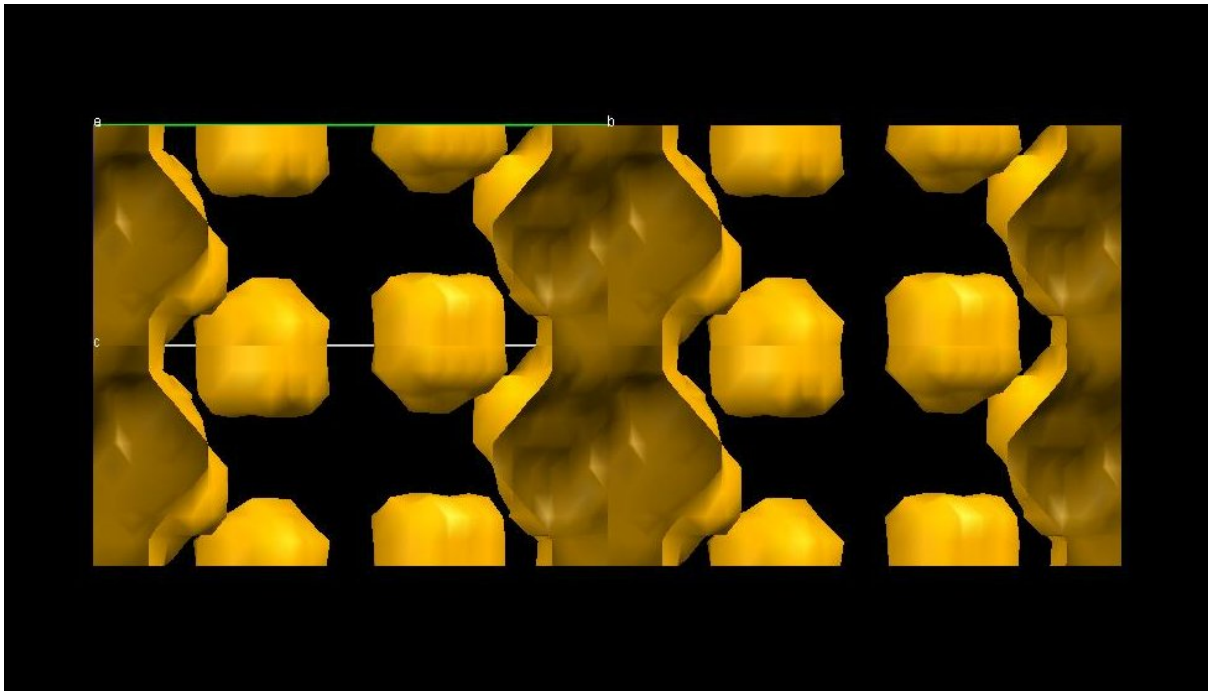

Figure S7. STAM-1_{MeOH} contact surface as calculated in MERCURY, viewed along the crystallographic *a*-axis. The hydrophobic pores can be seen centre, left and right. The previously hydrophilic channels are now seen as discrete pores with no permeability between them. Each spherical pore contains a disordered methanol molecule.

Compressibility of STAM-1_{MeOH} in MeOH

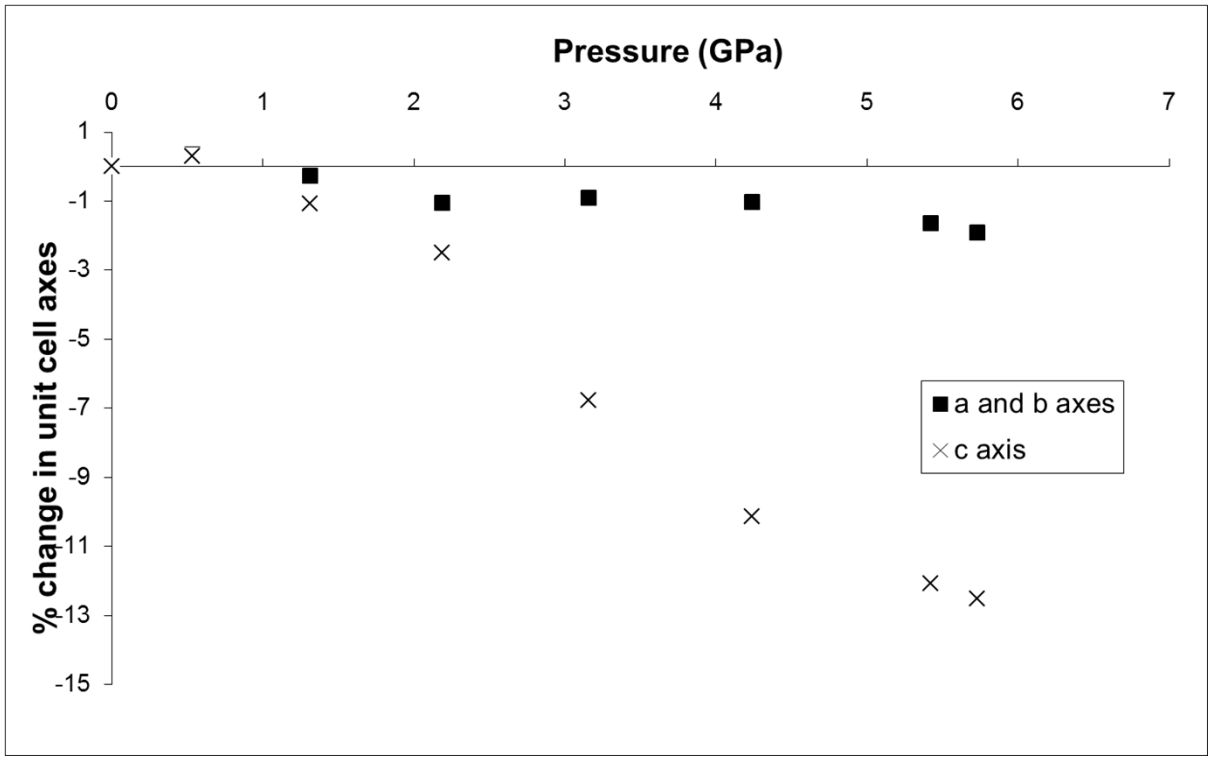

Figure S8. Unit cell *a/b*- (squares) and *c*-axis (crosses) length of STAM-1_{MeOH} in methanol as a function of pressure.

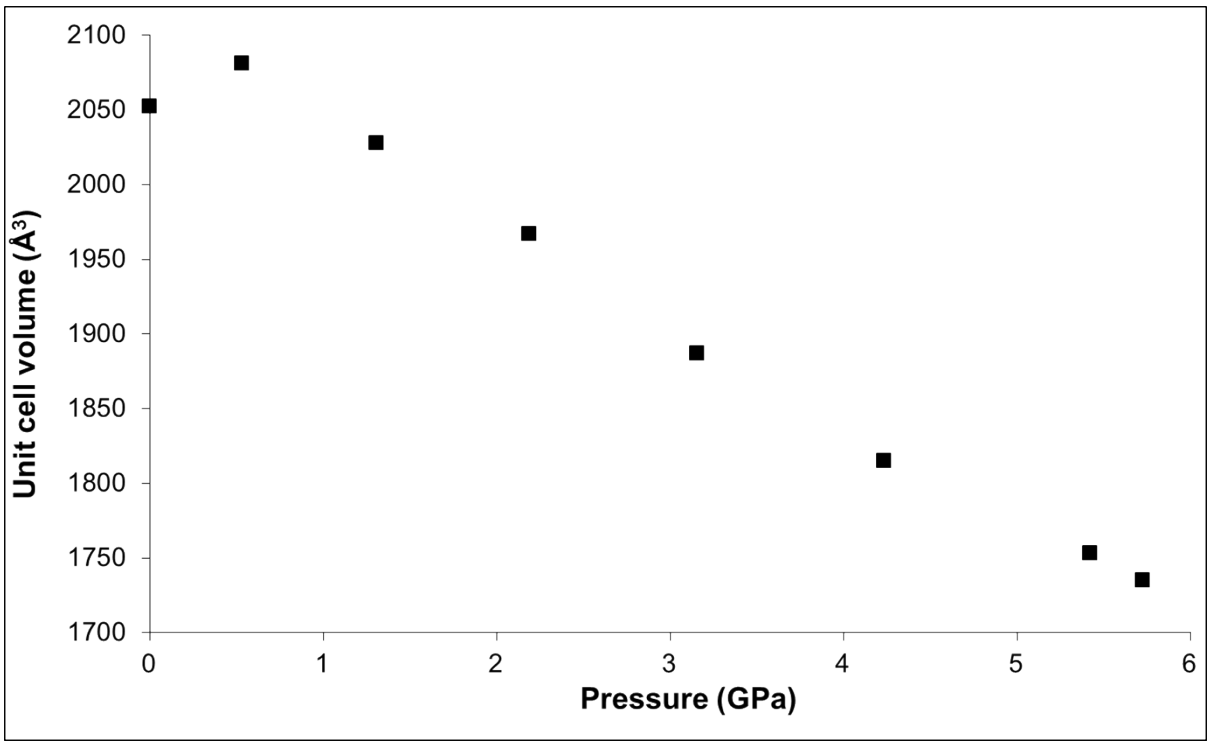

Figure S9. Unit cell volume of STAM-1_{MeOH} in methanol as a function of pressure.

Table S2. Pore volume and content statistics of STAM-1_{MeOH} in methanol as a function of pressure.

Pressure (GPa)	Hydrophobic pore		Hydrophilic pore	
	Volume (Å^3)	Electron count	Volume (Å^3)	Electron count
0.0	215	14	48	2
0.5	262	55	49	22
1.3	265	159	43	21

Compressibility of STAM-1 in IPA

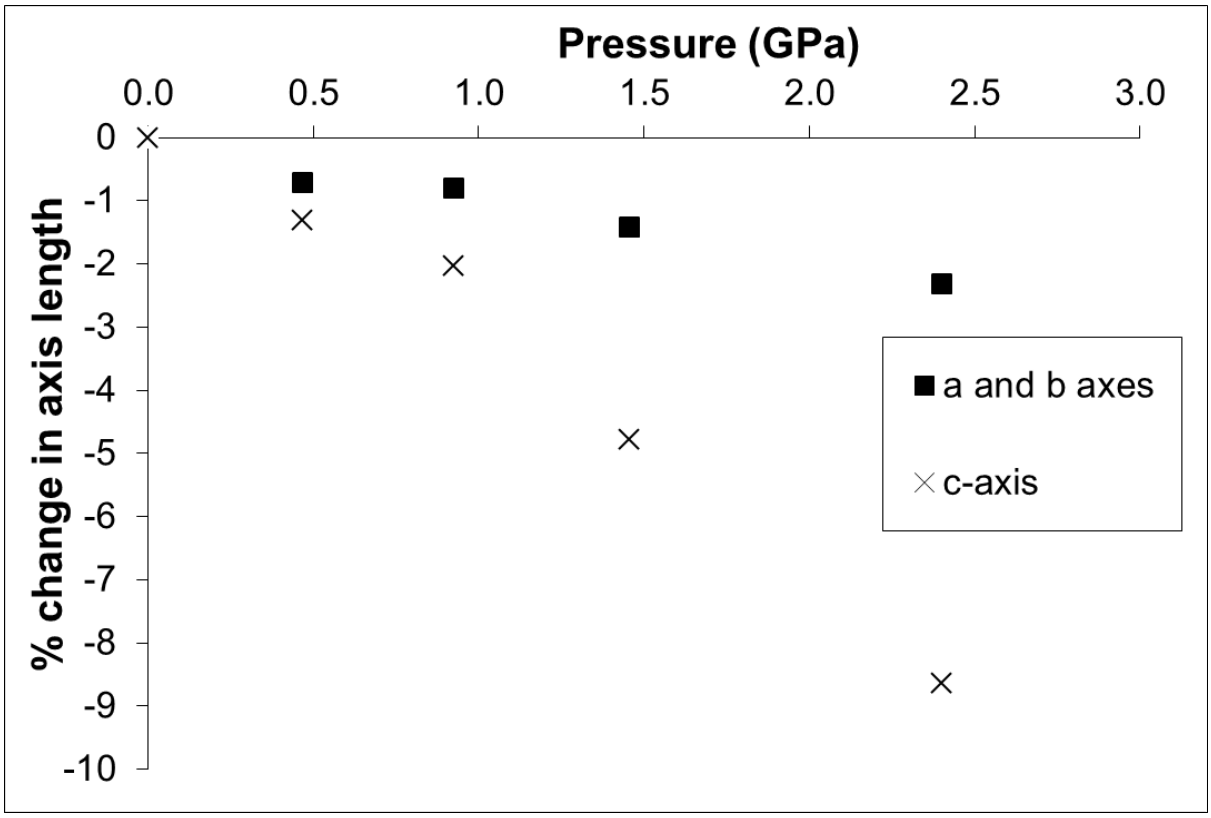

Figure S10. Unit cell *a/b*- (squares) and *c*-axis (crosses) length of STAM-1 in IPA as a function of pressure.

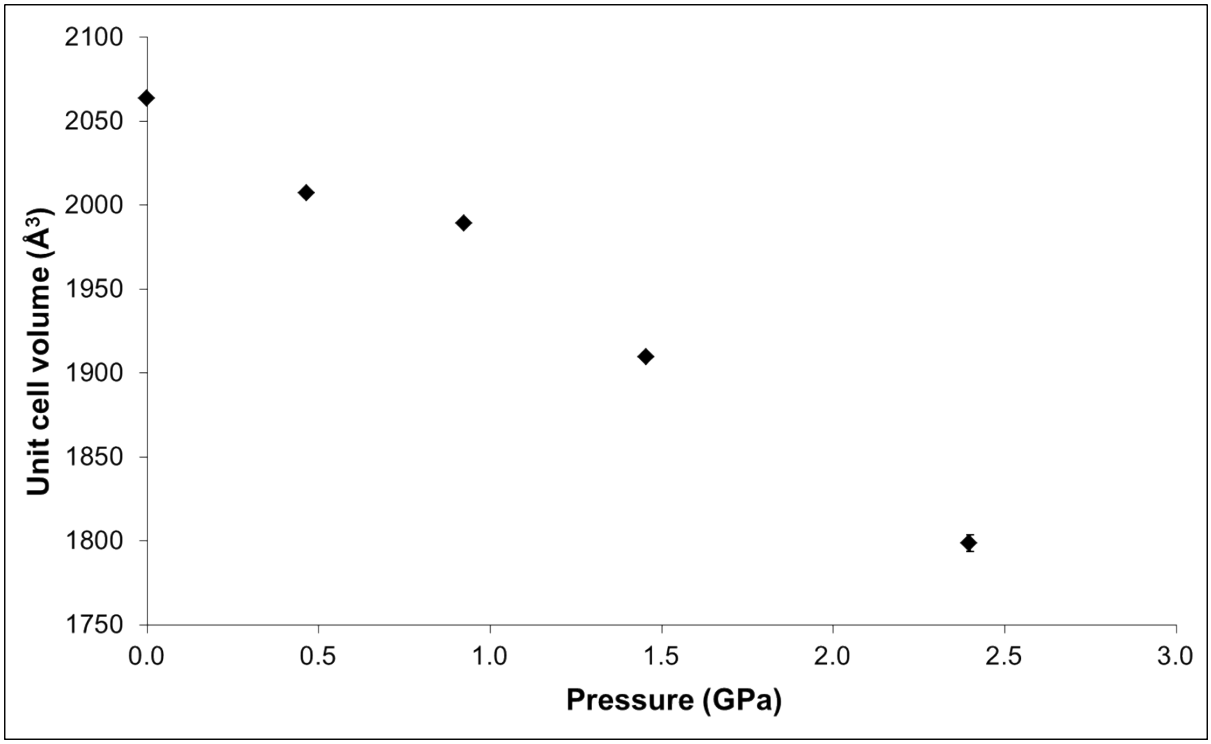

Figure S11. Unit cell volume of STAM-1 in IPA as a function of pressure.

Table S3. Pore volume and content statistics of STAM-1 in isopropyl alcohol as a function of pressure.

Pressure (GPa)	Hydrophobic pore		Hydrophilic pore	
	Volume (Å^3)	Electron count	Volume (Å^3)	Electron count
0.0	209	14	142	33
0.5	201	64	140	14
0.9	176	94	133	42

HKUST-1 vs STAM-1

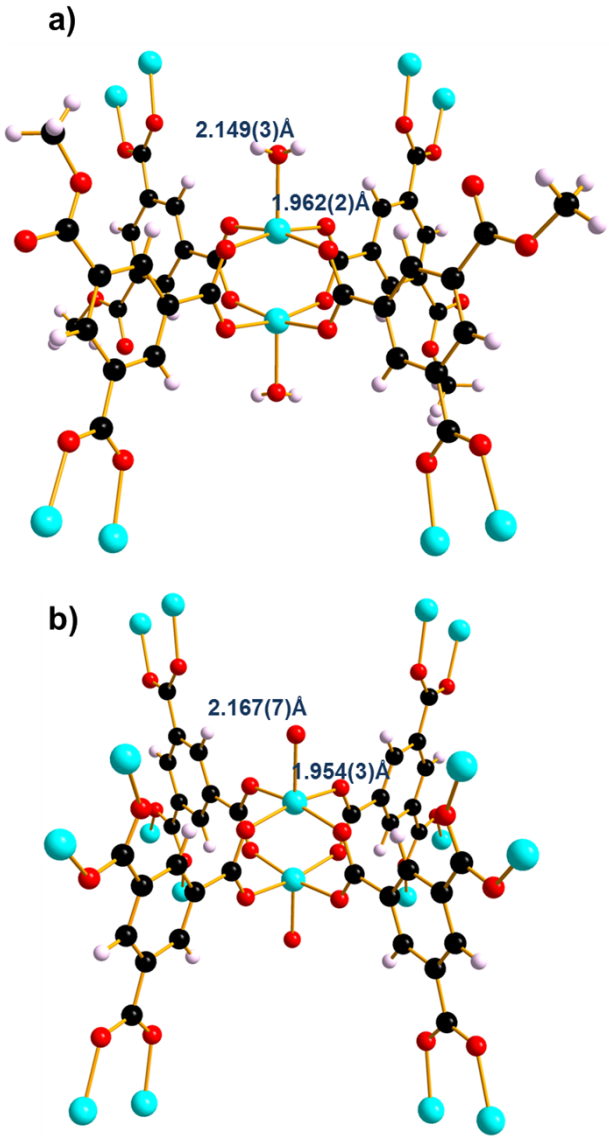

Figure S12 Comparison of Cu paddle wheel and directly bonded BTC linkers in **(a)** STAM-1 and **(b)** HKUST-1 (water H atoms not shown), with annotated bond distances for the axial and equatorial Cu-O bonds.

Structure of HKUST-1

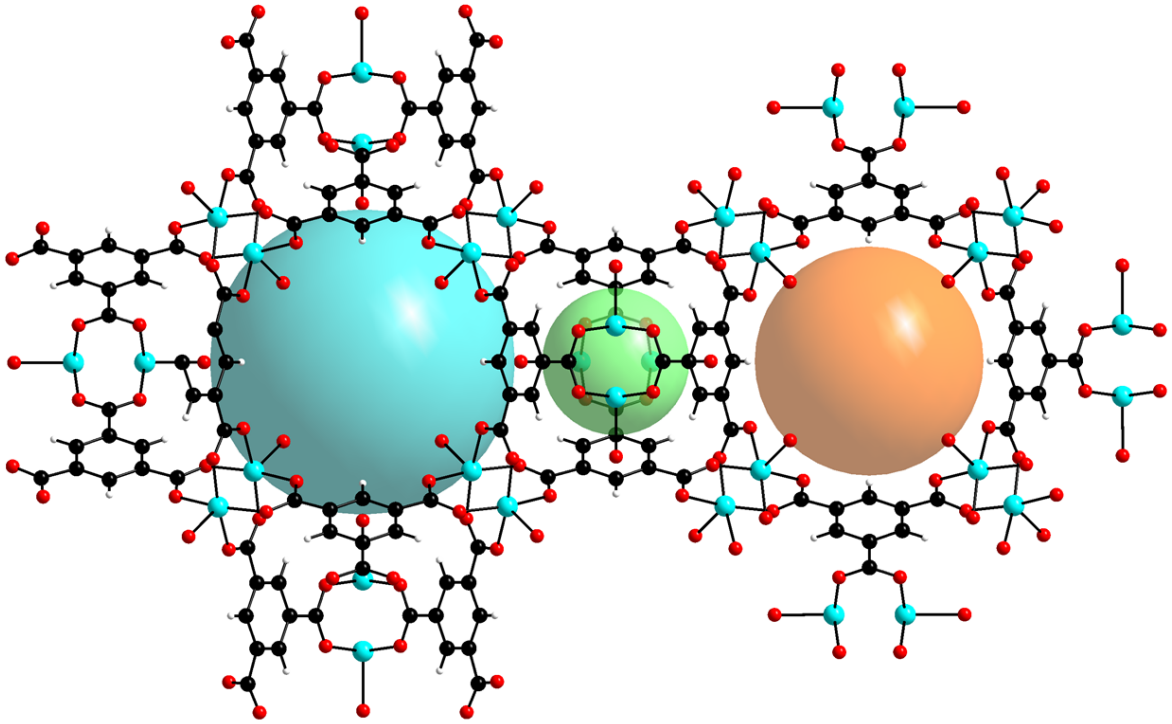

Figure S13. The three distinct but interconnected pores in HKUST-1. Guest-accessible cavities at (0,0,0) (blue), (½,½,½) (green) and (¼,¼,¼) (orange) are shown.

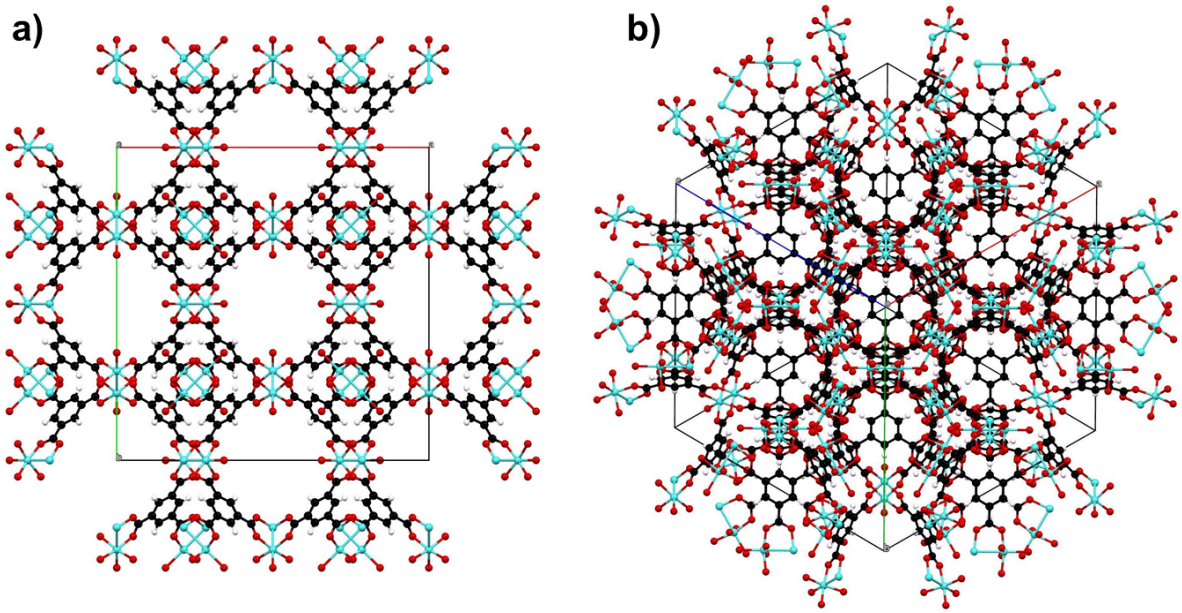

Figure S14. Packing of HKUST-1 viewed down along the (a) [0,0,1] and (b) [1,1,1] directions showing large central pores at (a) (0,0,0) and smaller 'capped' pores at (b) (¼,¼,¼).

Compressibility of STAM-1 in MeCHO

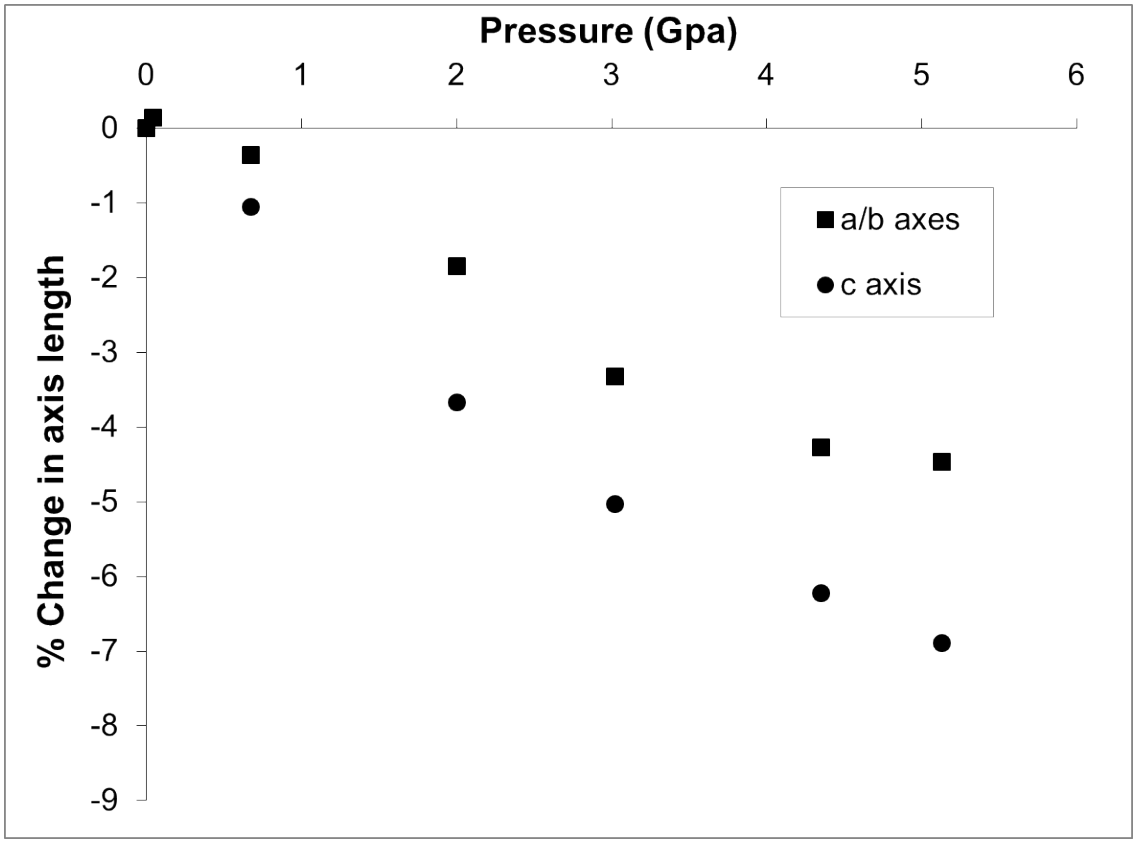

Figure S15. Unit cell *a/b*- (squares) and *c*-axis (circles) length of STAM-1 in MeCHO as a function of pressure.

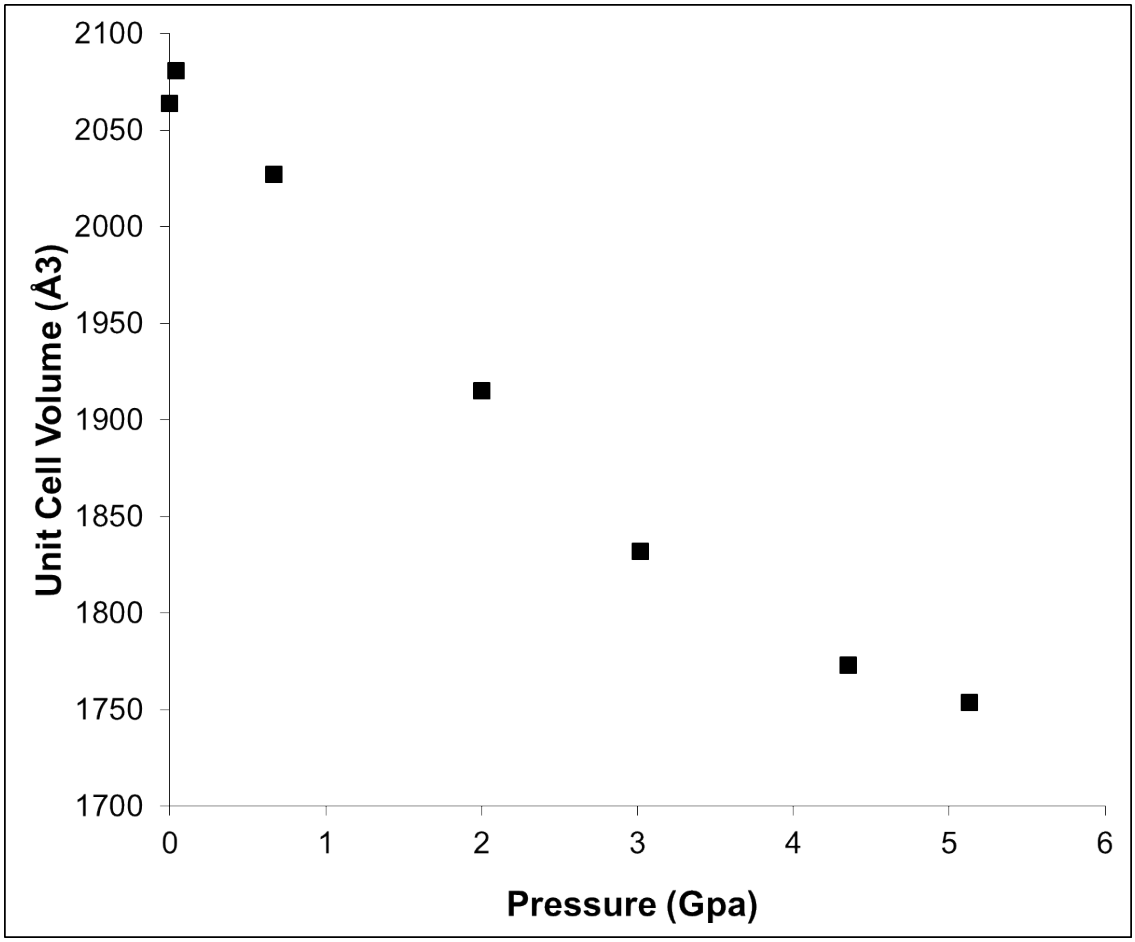

Figure S16. Unit cell volume of STAM-1 in MeCHO as a function of pressure.

Table S4. Void content statistics for the large hydrophobic pore and small hydrophilic pore of STAM-1_{MeOH} in MeCHO as a function of pressure with resolution cut to 1 Å, 1.2 Å and 1.5 Å.

Pressure (GPa)	e^- count (1 Å)		e^- count (1.2 Å)		e^- count (1.5 Å)	
	Large pore	Small pore	Large pore	Small pore	Large pore	Small pore
0.0	15	33	-	-	-	-
0.7	95	57	95	57	98	58
2.0	146	67	142	65	136	63
3.0	52	19	51	19	51	19

Structure of STAM-1_{MeNH2}

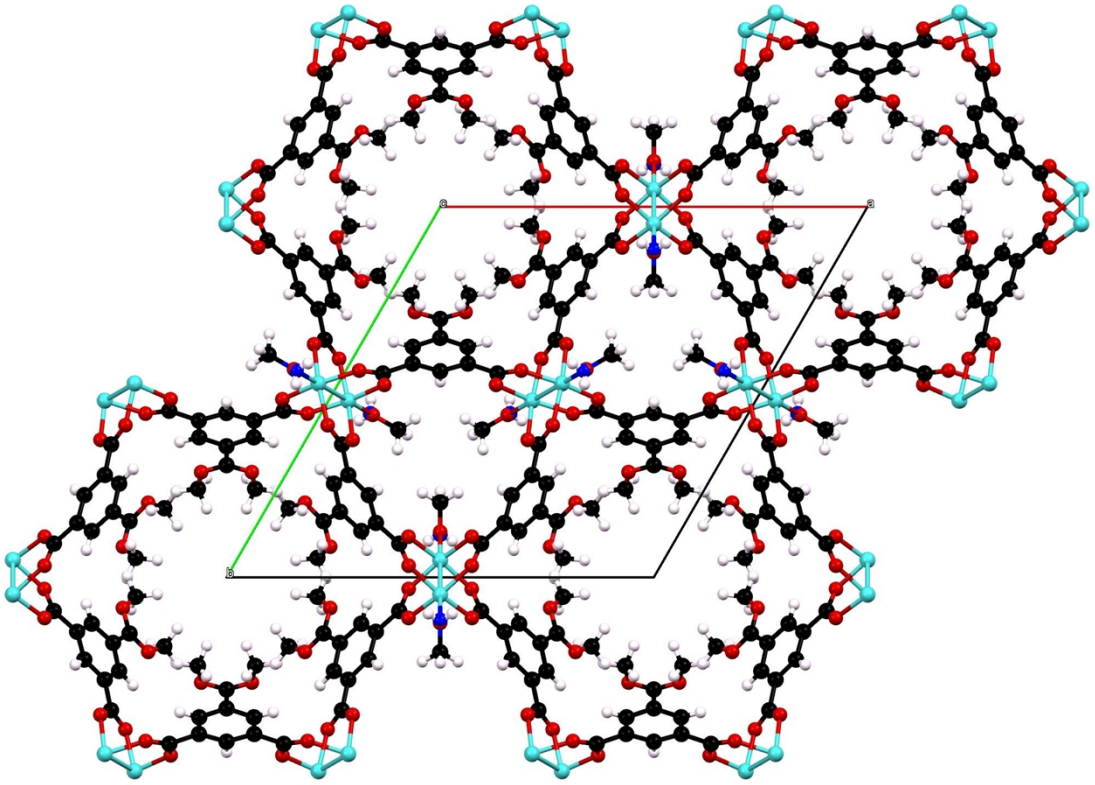

Figure S17. Structure of STAM-1_{MeNH2} viewed parallel to the crystallographic *c*-axis, showing the original hydrophobic channels lined by ester groups. The previously hydrophilic channels are now lined by one third-occupied methylamine ligands and two thirds-occupied water ligands.

Structure of STAM-1_{EtNH2}

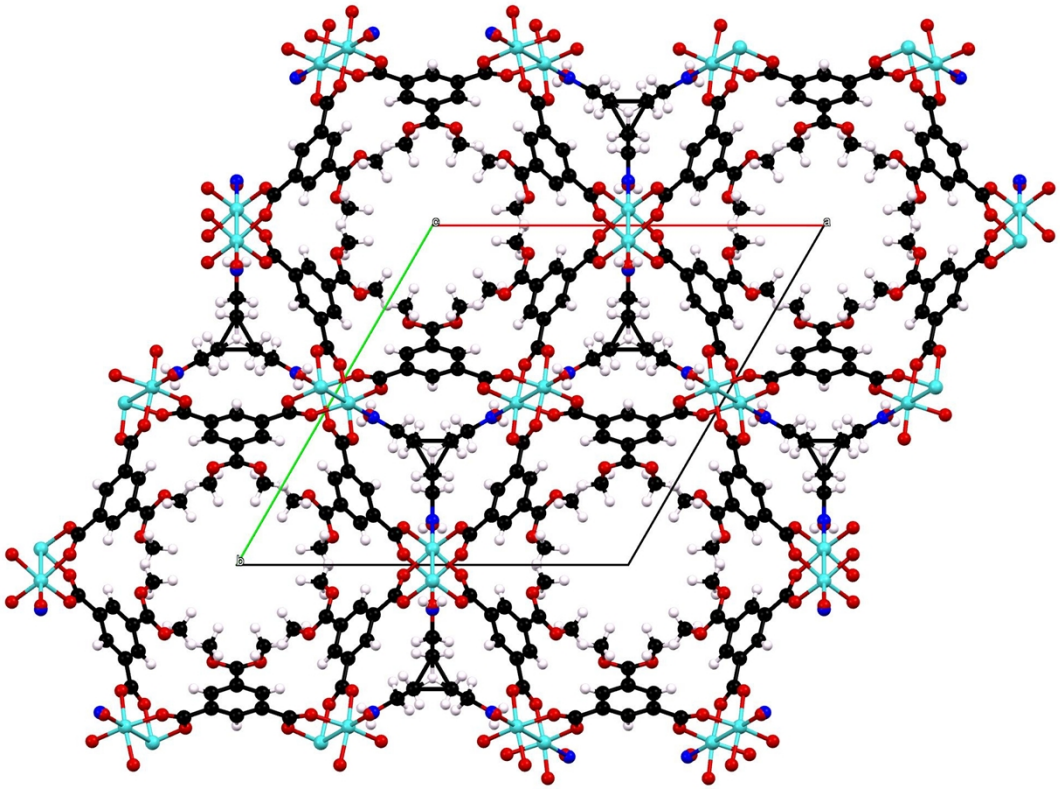

Figure S18. Structure of STAM-1_{EtNH2} viewed parallel to the crystallographic *c*-axis, showing the original hydrophobic channels lined by ester groups. The previously hydrophilic channels are now lined by one third-occupied ethylamine ligands and two thirds-occupied water ligands.

Table S5 Abridged crystallographic data and structure refinement parameters for STAM-1_{MeNH2} and STAM-1_{EtNH2}.

	STAM-1_{MeNH2}	**STAM-1_{EtNH2}**
empirical formula	$C_{33}H_{33}Cu_3N_1O_{21.5}$	$C_{32}H_{32}Cu_3N_1O_{22}$
temperature (K)	150(2)	150(2)
wavelength (Å)	0.71073	0.71073
crystal system	trigonal	trigonal
space group	$P\bar{3}m1$	$P\bar{3}m1$
a (Å)	18.626(3)	18.577(3)
b (Å)	18.626(3)	18.577(3)
c (Å)	6.8687(15)	6.8410(10)
α (°)	90	90
β (°)	90	90
γ (°)	120	120
volume (Å^3)	2063.8(7)	2044.5(5)
Z	2	2
density (g cm^{-3})	1.578	1.581
absorption coefficient (mm^{-1})	1.61	1.63
F(000)	998.0	988.0
θ range (°)	2.2 – 23.3	2.1 – 24.1
index ranges	$-17 \le h \le 0$	$-18 \le h \le 0$
	$0 \le k \le 20$	$0 \le k \le 21$
	$0 \le l \le 7$	$0 \le l \le 7$
reflections collected	6795	8199
independent reflections	1095 [*R*(int) = 0.094]	1203 [*R*(int) = 0.059]
data / restraints / parameters	1083 / 93 / 97	1193 / 103 / 100
goodness-of-fit on F^2	0.9342	0.8787
final *R* indices [$I > 2\sigma(I)$]	$R_1 = 0.062$	$R_1 = 0.061$
	$wR_2 = 0.136$	$wR_2 = 0.136$
R indices (all data)	$R_1 = 0.099$	$R_1 = 0.086$
	$wR_2 = 0.153$	$wR_2 = 0.150$
largest difference peak (eÅ^{-3})	1.48	1.92
deepest hole (eÅ^{-3})	-1.09	-1.57

Compressibility of STAM-1 in water

Table S6. Pore volume and content statistics of STAM-1 in water as a function of pressure.

Pressure (GPa)	Unit cell V (Å^3)	*a*/*b*-axis (Å)	*c*-axis (Å)	Hydrophobic pore		Hydrophilic pore	
				V (Å^3)	e$^-$ count	V (Å^3)	e$^-$ count
0.0	2058.2(4)	18.6500(17)	6.8329(9)	209	15	142	33
0.1	2071.5(4)	18.6230(20)	6.8973(7)	217	47	147	42

Compressibility of HKUST-1 in water

Table S7. Pore volume and content statistics of HKUST-1 in water as a function of pressure.

Pressure (GPa)	Unit cell V (Å^3)	*a*/*b*/*c*-axis (Å)	Total pore volume (Å^3)	e$^-$ count
0.0	18218.4(4)	26.313(3)	11615	1024
0.2	18333.8(14)	26.3684(12)	11816	2061
0.4	18329(7)	26.366(6)	N/A	N/A

References

1. M. I. H. Mohideen, B. Xiao, P. S. Wheatley, A. C. McKinlay, Y. Li, A. M. Z. Slawin, D. W. Aldous, N. F. Cessford, T. Düren, X. Zhao, R. Gill, K. M. Thomas, J. M. Griffin, S. E. Ashbrook and R. E. Morris, *Nat Chem*, 2011, **3**, 304-310.
2. S. S. Y. Chui, S. M. F. Lo, J. P. H. Charmant, A. G. Orpen and I. D. Williams, *Science*, 1999, **283**, 1148-1150.
3. S. A. Moggach, D. R. Allan, S. Parsons and J. E. Warren, *J. Appl. Crystallogr.*, 2008, **41**, 249-251.
4. G. J. Piermarini, S. Block, J. D. Barnett and R. A. Forman, *J. Appl. Physics*, 1975, **46**, 2774-2780.
5. Bruker-Nonius, Bruker-AXS, Madison, Wisconsin, USA, 2006.
6. G. M. Sheldrick, *SADABS Version 2008-1*, 2008.
7. P. W. Betteridge, J. R. Carruthers, R. I. Cooper, K. Prout and D. J. Watkin, *J. Appl. Crystallogr.*, 2003, **36**, 1487.
8. A. L. Spek, Utrecht University, Utrecht, The Netherlands, 2004.
9. P. W. Betteridge, J. R. Carruthers, R. I. Cooper, K. Prout and D. J. Watkin, *J. Appl. Crystallogr.* , 2003, **36**, 1487.
10. A. Dawson, D. R. Allan, S. Parsons and M. Ruf, *J. Appl. Crystallogr.*, 2004, **37**, 410-416.
11. S. Parsons, The University of Edinburgh, Edinburgh, United Kingdom, 2004.
12. A. J. Graham, J.-C. Tan, D. R. Allan and S. A. Moggach, *Chem. Commun.*, 2012, **48**, 1535-1537.
13. L. Palatinus and G. Chapuis, *J. Appl. Crystallogr.*, 2007, **40**, 786-790.
14. K. Brandenburg and H. Putz, Crystal Impact, Bonn, Germany, 2005.
15. C. F. Macrae, I. J. Bruno, J. A. Chisholm, P. R. Edgington, P. McCabe, E. Pidcock, L. Rodriguez-Monge, R. Taylor, J. van de Streek and P. A. Wood, *J. Appl. Crystallogr.*, 2008, **41**, 466-470.